

On the Internationalization of English Teaching System in the Planning of Sustainable Development of Future Renewable Energy

Xianfeng Liu¹

¹ Department of Public Course Teaching
Anhui Broadcasting Vocational College
Hefei, 230011 Anhui (China)
E-mail: 18756030628@163.com

Abstract. Energy is an essential element of human production and business activities. At present, China's energy development and utilization is facing the contradiction between increasing environmental pressure and high emission energy consumption structure. Based on the optimal power flow algorithm, this paper optimizes the scheduling and international teaching of the power system with a high proportion of renewable energy. The probability density function of fan output and photovoltaic output is obtained by wind speed and light intensity model, and the probability density function of load is also proposed. Then, interruptible load, microgrid and energy storage are used as flexible resources to improve the system's flexibility to meet the random fluctuations caused by a high proportion of wind and light, so as to maintain the stable operation of the power grid. The mathematical model of process optimization power flow satisfying process constraints is a nonlinear time-varying system. The key to process optimization power flow algorithm is to find a simple and effective linearization and discretization method that is in line with the actual power network. On the basis of ensuring the accuracy of the model, the theory, model and algorithm of the process optimization power flow are studied on the basis of the proposed linear time period, the approximate linear time variability of the node voltage, and the goal of greatly simplifying the problem. Finally, through simulation analysis, comparing the results of model 1 and model 2, we can see that from the point of view of the power abandonment cost, the power abandonment cost of model 1 is 2.29 million yuan, which is less than the 8 million yuan of model 2. From the perspective of depth peaking and start-stop times, the total depth peaking of model 1 is 331 times, which is greater than that of model 2, 258 times. The total start-stop of model 1 is 15 times, which is more than 9 times of model 2, so the total cost of optimized electricity of wind and light in model 2 is less than that in model 1. According to the optimal scheduling model of wind and light renewable energy, the effective utilization rate of renewable energy in China is low, and the teaching system should pay attention to this problem. Therefore, this paper puts forward an international English teaching strategy for the utilization rate of renewable energy.

Key words. Renewable Energy, Electric Power System, Optimized Power Flow Algorithm, A High Proportion, International Teaching.

1. Introduction

World energy, especially primary energy, has been shrinking with economic development, and environmental

pollution has become increasingly serious. China's national economy surpassed Japan in 2010, ranking second in the world, and has maintained a rapid growth rate in the past decade. In the future, China's national economy will maintain a high growth rate and have high requirements for energy, but the lack of energy and continuous exploitation have restricted the development of China's national economy [1]. Although China's installed capacity of wind power, hydropower and photovoltaic power generation ranks first in the world, China's renewable energy abandonment phenomenon is more serious than that of developed countries. In Germany, for example, wind power generation accounts for 6.5% of the total power generation in Germany, in the case of more wind power generation, its curtailment rate can be maintained at about 0.2%. China's grid-connected wind power generation is less than 3% of the total power generation, but the wind curtailment rate in 2016 was 43% in Gansu, 38% in Xinjiang, 30% in Jilin and 21% in Inner Mongolia. Although the wind curtailment rate decreased significantly in 2018, it still reached 8% on average. In order to improve the operational stability of the energy system with a high renewable energy penetration rate, renewable energy such as wind, light and water is required to cooperate with conventional energy, reduce the energy abandonment of renewable energy, and improve the reliable supply and use efficiency of energy [2].

Globally, renewable energy technology is rapidly becoming a key force in driving the transformation of the energy structure. With the rapid development in this field, the education sector has gradually recognized the importance of integrating renewable energy knowledge and technology into teaching strategies. The integration of renewable energy technology with teaching strategies enhances the core concept of sustainable development education, which emphasizes not only the rational use of natural resources but also innovation and development based on environmental protection. Students not only learn how to utilize natural resources but also how to innovate and develop in the context of environmental protection, which is of great significance for building an ecological civilization society.

At present, Guo Zhizhong et al. proposed an evaluation index of wind power on-grid power stability to measure the advantages and disadvantages of different scheduling strategies in compensating unbalanced power [3]. Colmenares-Quintero and others determined the teaching styles (TS) and learning styles (LS) of teachers and students in public schools, emphasizing renewable energy, and designed and applied course strategies based on active learning related to the Sustainable Development Goals (SDGs) [4]. Wang Chengshan et al. studied the winter operation optimization scheduling problem of an integrated energy system in an actual park. Based on detailed modeling of the equipment, they established a two-stage multi-time scale model predictive control scheduling strategy including rolling optimization and dynamic adjustment [5]. Xiao Hao et al. proposed a multi-time scale coordinated scheduling method based on model predictive control (MPC) to solve the problems that the traditional multi-time scale optimization scheme based on the flow section information is prone to such problems as the unit adjustment response is not timely and the planning tracking error is large [6].

Based on the linear time period algorithm of time-varying power flow, this paper studies the models and algorithms, and innovatively puts forward a process optimization power flow algorithm that is mathematically accurate without error and efficient and fast in application. Based on the optimal power flow algorithm, this paper optimizes the scheduling and international teaching of the power system with a high proportion of renewable energy. Interruptible load, microgrid and energy storage are used as flexible resources to improve the system's flexibility to meet the random fluctuations caused by a high proportion of wind and light, so as to maintain the stable operation of the power grid. The key to process optimization power flow algorithm is to find a simple and effective linearization and discretization method that is in line with the actual power network. On the basis of ensuring the accuracy of the model, the theory, model and algorithm of the process optimization power flow are studied on the basis of the proposed linear time period, the approximate linear time variability of the node voltage, and the goal of greatly simplifying the problem.

2. Renewable Energy Probability Model

A. Wind and Electricity Energy Probability Model

The main factor affecting wind power generation is wind speed. Generally speaking, the relationship between wind power and air density, fan blade radius, and wind speed can be expressed by equation (1):

$$P = \frac{1}{2} C_p(\lambda, \gamma) \pi \rho r^2 v^3 \quad (1)$$

Theoretically, the power-speed curve for different types of wind turbines is usually an "S"-shaped curve composed of sections for cutting in, climbing, and cutting out. Due to the influence of factors such as wind direction and atmospheric pressure, the actual output power of wind turbines may fluctuate around the theoretical curve [7]. There exists a nonlinear relationship between wind speed

and power output, and the distribution of power output fluctuations at different wind speeds is also different. Because the physical relationship between wind speed and power output is complex, the uncertainty in power output prediction cannot be characterized by existing probability distribution functions.

Light intensity is one of the main factors determining the power of photovoltaic power generation, and the light intensity of the sun over a period of time can be approximated as a Beta distribution:

$$f_{PV}(P_{PV}) = \frac{\Gamma(\alpha + \beta)}{\Gamma(\alpha)\Gamma(\beta)} \left(\frac{P_{PV}}{P_{PV \max}} \right)^{\alpha-1} \left(1 - \frac{P_{PV}}{P_{PV \max}} \right)^{\beta-1} \quad (2)$$

The output power of photovoltaic power generation has the following relationship with the light intensity:

$$P_{PV} = A\eta r \quad (3)$$

Where: A is the total area of the photovoltaic array; η is the photoelectric conversion efficiency of photovoltaic array; r is the light intensity. The randomness of light intensity leads to the random fluctuation of photovoltaic array output power.

B. Load Probability Model and Serialization Model

The load is also random, and normal distribution is usually used to describe the uncertainty of the load [8]. The probability density function of the load is:

$$f(P_L) = \frac{1}{\sqrt{2\pi}\sigma_L} \exp\left(-\frac{(P_L - \mu_L)^2}{2\sigma_L^2}\right) \quad (4)$$

The power output of power grid, photovoltaic output and load are random variables subject to different distributions respectively. According to the theory of sequence operation, the continuous probability distribution can be discretized to obtain the probabilistic sequence of random variables of a microgrid in each time period. To discretize its probability distribution, it is necessary to determine its distance length first. In order to facilitate the sequence operation, the following principles should be followed: variables of the same category should take the same discretization step; Each sequence for which the volume sum and volume difference operations will be performed shall take the same discretization step [9]. Therefore, the same value is selected for the discrete step size of wind power output, photovoltaic output and load.

Since the value range of wind power is $[0, P_{wr}]$, its cumulative probability distribution is not continuous, and it is discrete when the output is 0 and P_{wr} , so the discrete probabilities for $P_w=0$ and $P_w=P_{wr}$ should be considered when calculating the probability of the sequence. The probability sequence of wind power output is:

$$a(i_a) = \begin{cases} \int_0^{q/2} f_w(P_w) dP_w + f_w(0) & i_a = 0 \\ \int_{i_a q - q/2}^{i_a q + q/2} f_w(P_w) dP_w & 0 < i_a < N_w \\ \int_{i_a q}^{i_a q + q/2} f_w(P_w) dP_w + f_w(P_{wr}) & i_a = N_w \end{cases} \quad (5)$$

The method of obtaining the probability series of photovoltaic output and load is basically the same as that of wind power output. Since the $f_v(P_{pv})$ and $f_l(p)$ probability distributions are continuous, their probability sequences are shown in equations (6) and (7), respectively:

$$b(i_b) = \begin{cases} \int_0^{q/2} f_{pv}(P_{pv}) dP_{pv} & i_b = 0 \\ \int_{i_b q - q/2}^{i_b q + q/2} f_{pv}(P_{pv}) dP_{pv} & 0 < i_b < N_{pv} \\ \int_{i_b q}^{i_b q + q/2} f_{pv}(P_{pv}) dP_{pv} & i_b = N_{pv} \end{cases} \quad (6)$$

$$c(i_c) = \begin{cases} \int_0^{q/2} f(P_L) dP_L & i_c = 0 \\ \int_{i_c q - q/2}^{i_c q + q/2} f(P_L) dP_L & 0 < i_c < N_L \\ \int_{i_c q}^{i_c q + q/2} f(P_L) dP_L & i_c = N_L \end{cases} \quad (7)$$

C. Flexibility Index

In addition to quantifying system flexibility, the flexibility index can also exert flexibility constraints and effectively invoke flexibility resources [10]. The line capacity index reflects the flexibility demand of the line, and the net load fluctuation rate and the upper limit of the net load fluctuation rate reflect the fluctuation amplitude of the system net load and the ability of the system to cope with the net load fluctuation [11], [12].

The high proportion of wind and optical DG connected to the distribution network may cause local transmission congestion of the distribution line. In this paper, the capacity index of the distribution line is used to reflect the capacity margin of the distribution line, and is used as the flexibility index of the line.

$$D_{i,t}^{LCM} = \frac{P_{i,\max} - P_{i,t}}{P_{i,\max}} \quad (8)$$

The upper limit of net load fluctuation is the maximum adjustment capacity of the system when the distribution network is assigned to cope with the current random fluctuation, as shown below:

$$D_{i,\max}^{FRNL} = \frac{\sum_{i=1}^{N_{DG}} R_{i,t}^{DG} + \sum_{i=1}^{N_{cs}} R_{i,t}^{ess} + \sum_{i=1}^{n_{MG}} R_{i,t}^{MG} + R_{i,t}^S}{P_t^L} \times 10 \quad (9)$$

Net load fluctuation is a quantitative index to measure the fluctuation of net load per unit of time in a distribution network under the influence of a high proportion of wind

and light DG. As shown in equation (10) :

$$D_t^{FRNL} = \left| 1 - \frac{P_{t-1}^L}{P_t^L} \right| \times 100\% \quad (10)$$

When the dispatching time is t , $P_{MG,t,\text{out}}$ is the maximum output power of the microgrid to the distribution network, and $P_{MG,t,\text{in}}$ is the maximum output power of the distribution network to the microgrid.

$$\begin{cases} P_{MG,t,\text{out}} = P_{PV,t} + P_{WT,t} + P_{DE,\max} + P_{ESS,t,\text{out}} - P_{Load,t} \\ P_{MG,t,\text{in}} = P_{PV,t} + P_{WT,t} + P_{ESS,t,\text{in}} - P_{Load,t} \end{cases} \quad (11)$$

The maximum energy storage charge and discharge power are determined by the limit of its own power and the current SOC, as shown in equation (12).

$$\begin{cases} P_{ESS,t,\text{out}} = \min\left[P_{ESS,\max}, \frac{S_{OC,t} \cdot C_{ESS}}{\Delta t}\right] \\ P_{ESS,t,\text{in}} = -\min\left[P_{ESS,\max}, \frac{(1 - S_{OC,t}) \cdot C_{ESS}}{\Delta t}\right] \\ S_{OC,t} = S_{OC,t-1} - \frac{P_{ESS,t-1} \cdot \Delta t}{C_{ESS}} \end{cases} \quad (12)$$

3. High Proportion Wind and Light Energy Scheduling Based on Process Optimization Power Flow Algorithm

A. Time Equivalent Load Forecasting and Power Adjustment

Process optimization power flow is used for short-term or real-time generation planning. The equivalent load is oriented to the time process, and the equivalent load prediction is the basis of the generation plan [13]. The equivalent load forecasting period is a linear period. This chapter begins with the equivalent load forecasting to discuss the process optimization power flow problem.

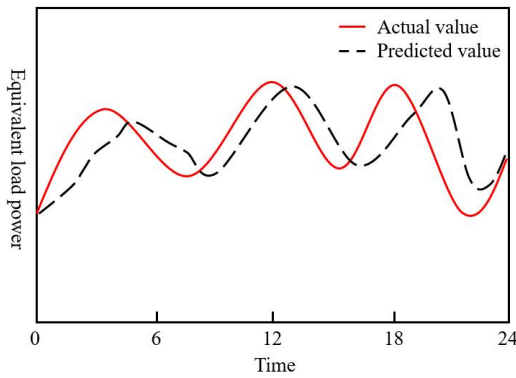
IPS has become or is becoming an important form of power supply for the grid. The load power has randomness, and the IPS power such as wind power and solar power has uncertainty. Randomness is a form of uncertainty. Load and IPS share the common characteristic of power uncertainty [14]. According to the idea of "merging similar items", this chapter regards IPS as a negative load, and merges load and IPS into equivalent load.

The load will not be easily cut, except for active loads: wind and solar power will not be easily abandoned, unless there is no willingness to make full use of renewable energy. The load power and IPS power are combined into equivalent load power, not only because of their commonality of power uncertainty, but also because of their similar position in the grid.

$$\forall t, \forall i: \begin{cases} P_i^e(t) = P_i^l(t) - P_i^{ips}(t) \\ Q_i^e(t) = Q_i^l(t) - Q_i^{ips}(t) \end{cases} \quad (13)$$

The equivalent load power is a continuous function of time. The equivalent load prediction is discrete, and the predicted result is the equivalent load on some equidistant time sections in the next scheduling cycle.

Predictions are always imperfect. Since the uncertainty in IPS power generation is significant, the forecast error for the aggregate load of a high percentage of renewable energy grids is much greater than that for traditional grids [15]. As the time scale changes, the forecast error for real-time scheduling is less than that for day-ahead scheduling. No matter what technological means are used, predictions can only reduce, but not completely eliminate, the forecasting errors of equivalent loads. Reducing forecasting errors has its limitations, especially for IPS power generation. When formulating electricity production plans, one must recognize and accept the existence of forecasting errors for equivalent loads.



The time period between adjacent prediction cross sections is the prediction period. The linear line formed by the predicted power of the two sections at the beginning and end of the prediction period is the equivalent load prediction line of the period, that is, the linear period. Therefore, no matter the power grid or any node, the linear prediction of the equivalent load in a time period has monotonicity [16]. The monotonicity here does not require that all nodes are consistent, and the slope of the equivalent load prediction line for the period is positive for some nodes and negative for some nodes.

For a short-term or real-time scheduling cycle, the time period equivalent load forecasting line is connected front to back and combined into the equivalent load forecasting line, that is, a linear period oriented to different time processes is formed, as shown in Figure 1.

Any predicted linear period is:

$$T_k \in [t_{k-1}, t_k] \quad (14)$$

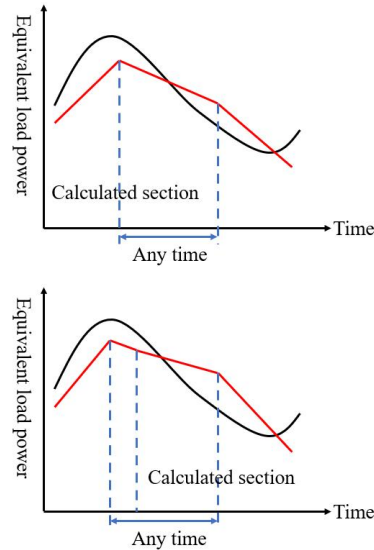


Figure 1. Equivalent Load Forecast Broken Line and Unbalanced Power in Time Segment

For each predicted linear period, the predicted power line of the first and last two sections is the predicted power line of the node equivalent load for the linear period.

$$\begin{cases} P_i^e(t) = P_i^e(t_k) + (t - t_k)W_{ik}^p \\ Q_i^e(t) = Q_i^e(t_k) + (t - t_k)W_{ik}^q \end{cases} \quad (15)$$

The node equivalent load forecast power line is synthesized into the total equivalent load forecast power line.

$$\begin{cases} P_{grid}^e(t) = P_{grid}^e(t_k) + (t - t_k)W_{grid,k}^p \\ Q_{grid}^e(t) = Q_{grid}^e(t_k) + (t - t_k)W_{grid,k}^q \end{cases} \quad (16)$$

When network power loss is ignored, the slope of the total equivalent load forecast power line is the sum of the slope of the node equivalent load forecast power line, i.e

$$\begin{cases} W_{grid,k}^p = \sum_{i=1}^n W_{ik}^p \\ W_{grid,k}^q = \sum_{i=1}^n W_{ik}^q \end{cases} \quad (17)$$

The above discussion shows that the predictive power of any forecast period and any node equivalent load is a linear function of time.

The formulation of power generation plan is to balance the equivalent load with a controllable power supply. Optimized power flow for specific calculated sections. In order to ensure the power balance of the non-calculated section, the power of the relevant power supply must be adjusted by means of peak regulation or frequency modulation, which is the power adjustment problem of the controlled power period in this section.

For each predictive linear period, the voltage amplitude of the controllable power supply changes very little, and it can be considered that the voltage amplitude of the controllable power supply node is constant. Therefore, this section does not deal with voltage amplitude adjustment [17].

To make a power generation plan based on the optimal power flow, a calculation section should be selected for each forecast linear period to calculate the optimal power flow. There is a power deviation between the non-calculated section and the calculated section, which is called the time unbalanced power. The calculation section is "point", the forecast period is "surface", and the period imbalance power is the result of "point with surface". The power imbalance varies with different sections, as shown in Figure 1. From the point of view of minimizing the power imbalance in the time period, the median section should be selected as the calculation section of optimized power flow.

The unbalanced power caused by the prediction error is unknown. The time period imbalance power is different from the other, and it has a known value. After the optimized power flow is calculated in the calculation section, the power of the controllable power supply must be adjusted in the non-calculation section in order to imbalance the power during the balance period. There are two ways to adjust: peak regulation and frequency modulation.

In the conventional power grid, real-time dispatching does not participate in the power balance process, and the task of unbalanced power during the balance period is jointly undertaken by the short-term dispatching peak regulating function and the AGC frequency regulating function.

High proportion of renewable energy grid, real-time dispatch participates in the power balance process. The period imbalance power of short-term generation plan is borne by the peak regulation function, and the period imbalance power of real-time generation plan is borne by the frequency modulation function of AGC.

Peak regulation of power grid is part of short-term power generation plan [18]. According to the fluctuation of the total equivalent load of the power grid, the dispatching center makes the peaking plan for generation following. When the total equivalent load increases, the generating power of the peaking unit is increased, and the generating power of the peaking unit is reduced. Generally speaking, there will not be some improvement and some reduction. It is reasonable to think that the power adjustment of power network peak regulation is time monotonic.

B. Process Optimization Power Flow

The continuation of time-optimized flow forms process-optimized flow (POPF), and time-optimized flow is the basis of process-optimized flow. Combined with the research on the optimal dispatch of high-proportion renewable energy power grid, the verification of numerical examples will be given in the next chapter.

The objective function of the median cross-section is optimized by time-optimized power flow. The median section has an energy background, so the economy of the characterization period is more reasonable.

Since the approximate linear relationship between node voltage and time is guaranteed, the two extreme operating conditions of the linear period are bound to appear on the first and last two sections, which meet the constraints, meaning that all sections within the period meet the constraints [19]. According to the frequency modulation characteristics of the power network, the inequality constraints of power and voltage are checked in two boundary value sections.

Obviously, based on the concept of linear period, the time-optimized power flow simplifies the continuous time optimization model of each period into the time-optimized model of three characteristic cross sections, which greatly simplifies the mathematical model of time-optimized power flow.

The three-section period optimization model is detailed as follows.

Median cross-section objective function:

$$\forall T_k : \min f(\mathbf{U}, \mathbf{X}, t_k^m) \quad (18)$$

Median cross-section constraints:

$$\forall T_k : \mathbf{h}(\mathbf{U}, \mathbf{X}, t_k^m) = 0 \quad (19)$$

Boundary value cross-section constraints:
The power flow equation constraint is

$$\forall T_k : \begin{cases} \mathbf{h}(\mathbf{U}, \mathbf{X}, t_{k-1}) = 0 \\ \mathbf{h}(\mathbf{U}, \mathbf{X}, t_k) = 0 \end{cases} \quad (20)$$

The voltage inequality constraint is

$$\forall T_k : \begin{cases} \mathbf{V}_{\min} \leq \mathbf{V}(t_{k-1}) \leq \mathbf{V}_{\max} \\ \mathbf{V}_{\min} \leq \mathbf{V}(t_k) \leq \mathbf{V}_{\max} \end{cases} \quad (21)$$

The power inequality constraint is

$$\forall T_k : \begin{cases} \mathbf{P}_{\min^c} \leq \mathbf{P}^c(t_{k-1}) \leq \mathbf{P}_{\max^c} \\ \mathbf{Q}_{\min^c} \leq \mathbf{Q}^c(t_{k-1}) \leq \mathbf{Q}_{\max^c} \\ \mathbf{P}_{\min^c} \leq \mathbf{P}^c(t_k) \leq \mathbf{P}_{\max^c} \\ \mathbf{Q}_{\min^c} \leq \mathbf{Q}^c(t_k) \leq \mathbf{Q}_{\max^c} \end{cases} \quad (22)$$

The line power inequality constraint is

$$\forall T_k : \begin{cases} \mathbf{P}^{\text{line}}(t_{k-1}) \leq \mathbf{P}_{\max^{\text{line}}} \\ \mathbf{P}^{\text{line}}(t_k) \leq \mathbf{P}_{\max^{\text{line}}} \end{cases} \quad (23)$$

Traditional optimal flow algorithms, such as the Newton-Raphson method and the gradient method, perform well in computational speed and accuracy, but they often exhibit slow convergence speeds and a tendency to get stuck in local optima. Additionally, these algorithms may encounter difficulties when dealing with large-scale grids or complex constraint conditions.

The time-optimized power flow is an optimal power flow about the median cross section which satisfies the time-period inequality constraint. The time period optimization power flow algorithm is mainly composed of median optimization and boundary value constraint check.

1) Median Section Optimization

The Newton method and the interior point method dealing with inequality constraints significantly improve the reliability and efficiency of optimal power flow calculation, which is of milestone significance for the development and perfection of optimal power flow algorithm. In this chapter, a combination of the above two methods is used to calculate the optimal power flow of the median section. There is much literature on the optimization of power flow by Newton's method, the optimization of power flow by the interior point method and their combination. As this part of the content does not belong to the innovation of this paper, do not take up space to describe.

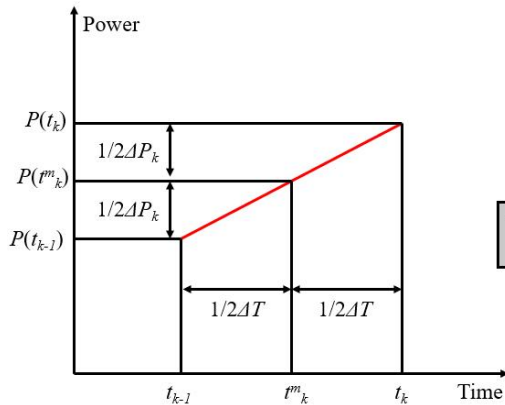


Figure 2. The Basic Flow Chart of the Optimized Power Flow Algorithm for Time Period

Based on the fact that the working conditions of adjacent periods are close, this chapter takes the optimization result of the median section of the previous period as the initial value of the optimization of the median section of the next period, namely

$$\begin{cases} \mathbf{P}_0^c(t_k^m) = \mathbf{P}^c(t_{k-1}^m) \\ \mathbf{V}_0^c(t_k^m) = \mathbf{V}^c(t_{k-1}^m) \end{cases}, (k = 1, 2, \dots, N) \quad (24)$$

C. Optimal Dispatching Model of Wind and Light Distribution Network with High Proportion

In this paper, interruptible load, microgrid and energy storage are used as flexible resources to participate in system regulation, and an optimal scheduling model with minimum net load fluctuation and operating cost as objective functions is constructed. Because the objective function is different in dimension and index value,

2) Boundary Value Constraint Check

Based on the optimization results of the median cross-section, it is adjusted according to the linearized controllable power supply adjustment mode of peak regulation or frequency modulation.

The power generation of the controlled power supply is integrated, and the power flow of the two boundary value sections is calculated to check the two extreme conditions of the boundary value sections. If neither boundary value section violates the constraint, the period optimization power flow calculation ends. Otherwise, it is necessary to adjust the power limit of the controllable power supply according to the violation of voltage constraint, and iteratively calculate the optimal power flow of the median cross-section until the boundary value cross-section meets the constraint check [20]. If the boundary value section constraint check cannot be satisfied no matter how adjusted, the solution closest to the boundary condition should be selected as the optimal solution.

3) Basic Flow Chart

Figure 2 is the basic flow chart of the time-optimized power flow algorithm.

dimensionless processing is performed on it first [21]. In order to achieve effective scheduling of flexible resources in a distribution network, this paper combines the analytic hierarchy process (AHP) and entropy weight method, and uses a comprehensive index method to determine the weight.

$$w_{Sy-i} = \frac{w_{AHP-i} + w_{EM-i}}{\sum (w_{AHP-i} + w_{EM-i})} \quad (25)$$

$$\min F = \min \{w_{Sy-1}F_1' + w_{sy-2}F_2'\} \quad (26)$$

In order to suppress the net load fluctuation of the distribution network and improve the system flexibility, objective function 1 selects the minimum net load fluctuation index as the optimization object, as shown below:

$$F_1 = \sum_{t=1}^T D_t^{\text{FRNL}} \quad (27)$$

The total operation cost of this paper includes the network loss cost of the distribution network, the power purchase cost of the grid, the operation cost of energy storage, the cost of energy interaction between the microgrid and the distribution network, and the compensation cost of the interrupted load. The objective function 2 is shown in equation (28) below

$$F_2 = \sum_{t=1}^T \left[\rho_t P_t^{\text{loss}} + \rho_t P_t^{\text{grid}} + \sum_{i=1}^{N_{\text{LL}}} m_c^{\text{IL}} P_{i,t}^{\text{IL}} + B(t) + \sum_{i=1}^{N_{\text{ESS}}} K_i^{\text{ESS}} \right] \quad (28)$$

Power flow constraints:

$$\begin{cases} P_{i,t} = U_{i,t} \sum_{j=1}^N U_{j,t} (G_{ij} \cos \theta_{ij} + B_{i,j} \sin \theta_{ij}) \\ Q_{i,t} = U_{i,t} \sum_{j=1}^N U_{j,t} (G_{ij} \sin \theta_{ij} - B_{i,j} \cos \theta_{ij}) \end{cases} \quad (29)$$

Node voltage constraints:

$$U_{i,\min} \leq U_{i,t} \leq U_{i,\max} \quad (30)$$

Reactive power balance constraints:

$$Q_t^{\text{grid}} + \sum_{i=1}^{N_{\text{DG}}} Q_{i,t}^{\text{DG}} + \sum_{i=1}^{N_{\text{LL}}} Q_{i,t}^{\text{IL}} = \sum_{i=1}^N Q_{i,t} \quad (31)$$

Active power balance constraints:

$$P_t^{\text{grid}} + \sum_{i=1}^{N_{\text{DG}}} P_{i,t}^{\text{DG}} + \sum_{i=1}^{N_{\text{MG}}} P_{\text{MG},i,t} + \sum_{i=1}^{N_{\text{LL}}} P_{i,t}^{\text{IL}} + \sum_{i=1}^{N_{\text{ESS}}} P_{i,t}^{\text{loss}} = \sum_{i=1}^N P_{i,t} + P_t^{\text{loss}} \quad (32)$$

4. Simulation Analysis

A. Comparative Analysis of Renewable Energy Optimization Models

In order to explain the rationality of the optimization results of the model, the comparison model is added. The comparison model is the minimum electricity cost model of wind optimization and the minimum total abandoned electricity cost model. The typical daily optimal output process of the three models is shown in Figure 3, and the optimal results are shown in Table 1. The frequency of depth peak regulation and the frequency of start and stop are shown in Table 2, and the optimal electrical peak regulation capacity of wind and light is shown in Table 3. In order to facilitate the comparative analysis, the total cost minimum model of wind, light optimization electricity cost

minimum model, and total abandoned power cost minimum model are referred to as model 1, model 2, and model 3.

Firstly, by comparing the results of Model 1 and Model 2, it is known that the abandonment cost of Model 1 is 229 million yuan, which is less than the 800 million yuan of Model 2. In terms of the depth of adjustment and the number of starts and stops of wind and solar optimization plants, Model 1 totals 331 adjustments, which is more than the 258 adjustments of Model 2. The total shutdowns of both models are 15 and 9, respectively. Therefore, the overall costs of Model 1 are lower than those of Model 2. From the perspective of water, wind, and solar optimization, the peak adjustment amplitude of Model 2 is 339.5 MW, which is less than the 365.5 MW of Model 1. Since Model 2 is more focused on optimizing the economic operation of wind and solar power stations, it attempts to minimize the adjustment depth and the frequency of deep adjustments and starts and stops. However, this increases the burden on hydropower stations for peak regulation. Therefore, the overall costs of Model 1 are lower than those of Model 2.

Then, comparing the results of model 1 and model 3, it can be seen that from the point of view of the power abandonment cost, model 3's power abandonment cost of 0 indicates that the power system can theoretically absorb all the power generation of water, wind and optical power stations. From the perspective of depth, peaking times and start-stop times, the total depth peaking times of model 3 is 367 times, which is greater than that of model 1, and the total start-stop times of 84 times is also greater than that of model 1. From the perspective of the electricity peak adjustment amplitude optimized by water wind and light, the hydropower peak adjustment amplitude of model 3 is 6.48 million kW, which is smaller than the hydropower peak adjustment amplitude of model 1 is 6.63 million kW, while the electricity peak adjustment amplitude optimized by wind and light of model 3 is 4.035 million kW, which is larger than model 1. Model 3 is more inclined to optimize the output process of water, wind and optical power stations to maximize the total absorbed electricity.

However, since the wind and light power stations have no adjustment capacity, although the hydropower station has an adjustment capacity, the typical daily available electricity consumption is relatively high. If the power is fully absorbed, the peak load capacity of the hydropower station will be greatly reduced, and the peak load range of the wind and light optimization power station will be increased, resulting in the wind and light optimization motor being in deep peak load or frequent start and stop state for a long time, and the cost of peak load and start and stop will be greatly increased. Therefore, although the abandoned power cost of model 3 is 0, the total cost is greater than that of model 1.

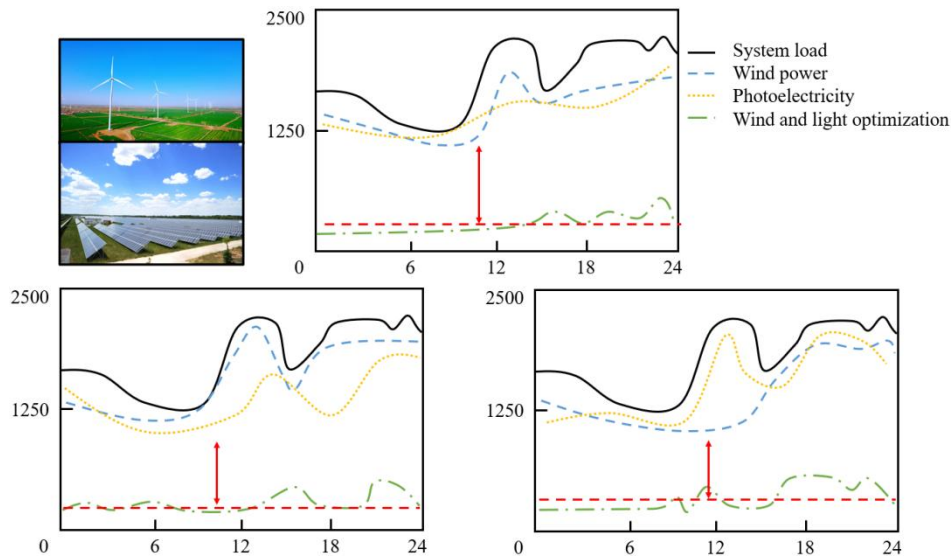


Figure 3. Optimal Output Process of the Model

Table 1. Comparison of Optimal Results of Different Models

MODEL	VARIOUS COSTS						Total cost
	Peak adjustment	Start-stop	Sewage	Curtailment	Obsolescence	Waste water	
Model 1	3742	256	1436	0	0	229	5663
Model 2	3554	152	1586	0	0	800	6093
Model 3	3984	1782	1463	0	0	0	7228

Table 2. Comparison of Electric Depth Peak Regulation and Start-stop Times Optimized by Wind and Light in Different Models

PROJECT	MODEL	CLASS I UNIT	CLASS II UNIT	CLASS III UNIT	CLASS IV UNIT	CLASS V UNIT
Depth peaking	Model 1	112	123	27	69	331
	Model 2	69	68	61	60	258
	Model 3	92	91	96	88	367
Start-stop number	Model 1	0	3	1	11	15
	Model 2	0	0	3	6	9
	Model 3	13	35	15	21	84

Table 3. Comparison of Wind and Light Optimization of Peak Regulation in Different Models

MODEL	WIND POWER			PHOTOELECTRICITY		
	Maximum output	Minimum output	Amplitude of peak regulation	Maximum output	Minimum output	Amplitude of peak regulation
Model 1	1546	882	664	650	284	366
Model 2	1546	843	703	650	311	339
Model 3	1546	897	649	650	247	403

From the comparison and analysis results of the models, it can be seen that the optimal operation mode of wind and light is closely related to the power abandonment cost and the total system cost. Therefore, the following scenario is set for comparative analysis to explain the relationship between the three scenarios: Scenario 1: On the basis of model 1, regardless of wind and light optimization of electrical depth peak load, that is, the minimum output of basic parameter stroke and optical optimization of the unit is uniformly set to the minimum technical output. Scenario 2: On the basis of model 1, the minimum continuous start-stop time of the basic parameter stroke and optically optimized generator unit is uniformly set as the total number of time periods in the scheduling period, regardless of wind and light optimization. Scenario 3: Based on

model 1, depth peak balancing and start-stop peak balancing are not considered at the same time. Figure 4(a) and (b) shows depth peak regulation and start-stop frequency of model 1, and Figure 4(c) and (d) shows the start-stop peak regulation frequency of scenario 1 and depth regulation frequency of scenario 2.

First of all, theoretically, deep peak regulation can expand the range of wind and light optimization power output, which is beneficial for power systems with large load peak valley differences. The results of Model 1 were compared with those of scenario 1, because the group was not allowed to carry out deep peaking due to the artificial setting of wind and light-optimized motors in scenario 1, the ability of wind and light-optimized electric peaking

decreased, although the start-stop times were the same as those of model 1. However, due to different start-stop strategies, the cost of power abandonment increases. Therefore, the start-stop cost, power abandonment cost and

total cost of scenario 1 are all greater than that of model 1, indicating that deep peak regulation is conducive to reducing the power abandonment and total cost of the system.

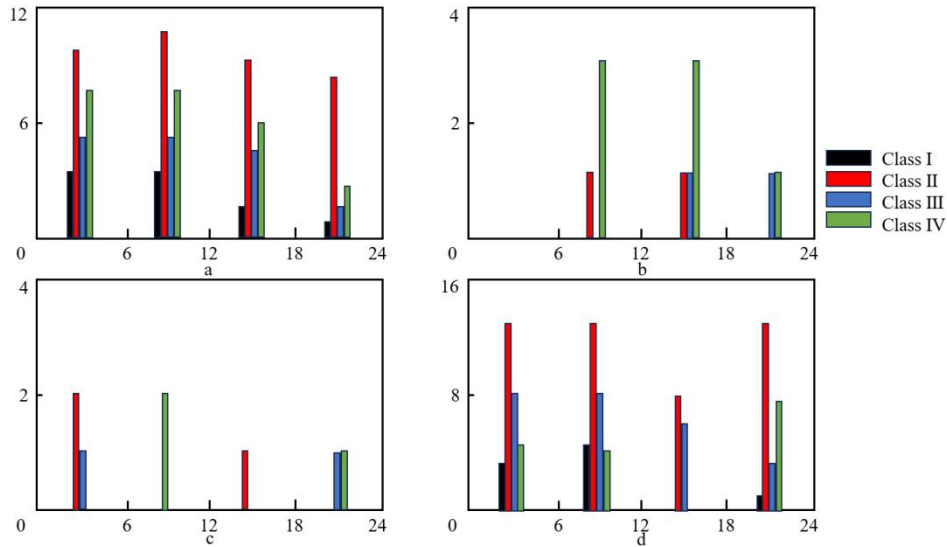


Figure 4. Depth Peak Load and Start-stop Times

Secondly, it takes a long time and complicated technology to change the start and stop state of the wind and optical optimization unit, so under normal circumstances, the unit is put into operation one day, and it is not allowed to shut down during the scheduling period. However, it is closely related to economic operation when the target power grid lacks a peaking power station. The results of model 1 are compared with those of scenario 2. In scenario 2, the change of start-stop state is not allowed due to the artificial setting of wind and light optimization units. Therefore, the start-stop cost of wind and light optimization in scenario 2 is 0, which is less than model 1. However, due to the lack of start-stop peak balancing, wind and light optimization electricity can only rely on the output of the opening unit for climbing and descending the peak balancing. It also leads to the decrease of peak load balancing capacity of wind and light-optimized generator units, and the unit is in

the state of deep peak load for a long time, and the total depth peak load is 390 times, which is greater than model 1, and the power abandonment cost increases. Therefore, the peak load balancing cost, power abandonment cost and total cost of scenario 2 are all greater than that of model 1, indicating that reasonable arrangement of wind and light-optimized power units to start and stop peak load balancing is also conducive to reducing the water landscape power abandonment cost and total system cost.

B. Load Variation and Tidal Current Direction

Figure 5 shows the response of the process optimization power flow algorithm and the distribution network and the end-user network connected by the process optimization power flow algorithm under the condition of uneven load change on the user side.

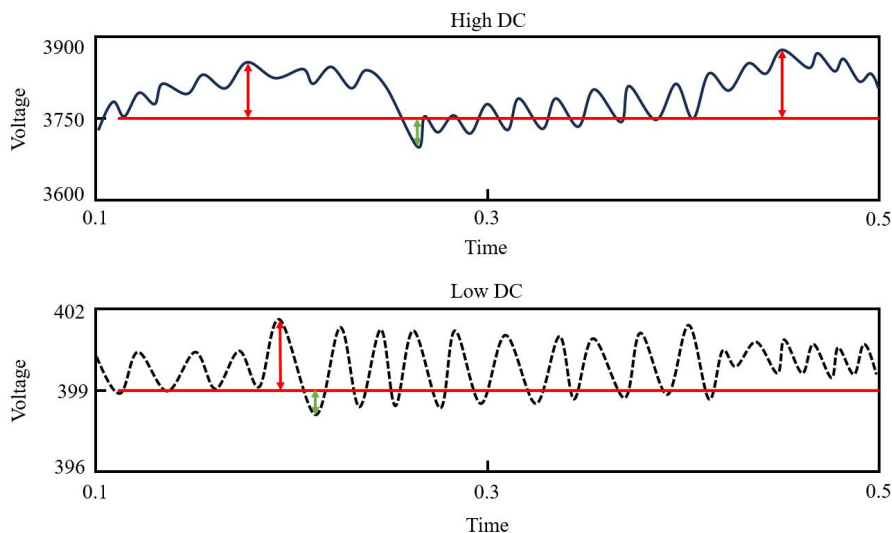


Figure 5. DC Side Voltage When the Load Changes

As can be seen from Figure 5, when the user-side load suddenly increases, the DC voltage of both the high

voltage side and the low voltage side changes. The user side load suddenly increases, and the system appears instantaneous power imbalance. As a result, the DC voltage on the high voltage side drops slightly, and after a period of oscillation below the rated voltage of 3800V, it returns to around 3800V. The DC voltage on the low-voltage side drops slightly at the low point of the first cycle, and then oscillates around the rated voltage of 400V. It can be seen that the oscillation amplitude is large, which can be

understood as the reactive power demand on the load side is provided by the low-voltage side at this time.

Figure 6 shows the response of the distribution network connected by the process optimization power flow algorithm and the end-user network when the output power of the user-side power supply system is greater than the user-side load.

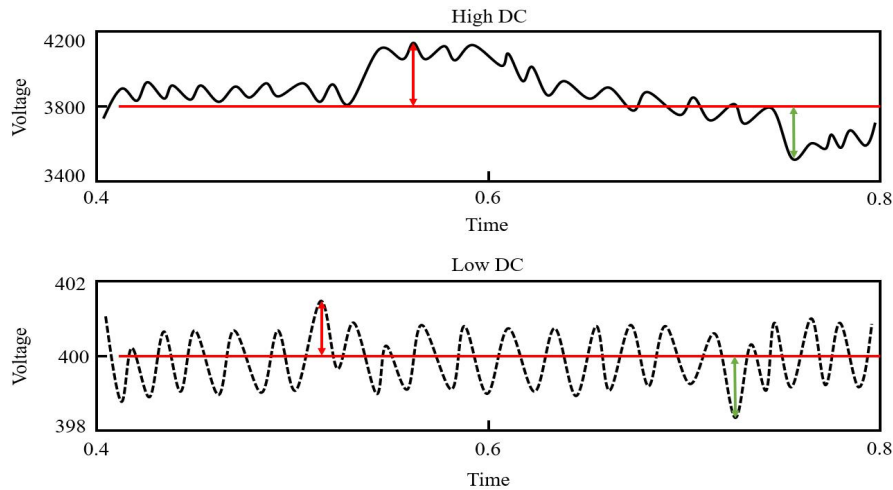


Figure 6. DC Voltage Waveform When the Power Flow is Reversed

As can be seen from Figure 6, when the output power of the power supply system at the user side is greater than the load at the user side, the DC voltage at both the high and low voltage sides changes. The user-side load suddenly changes from positive to negative, and instantaneous excess power occurs in the system. Therefore, the DC voltage on the high voltage side rises slightly, and after a period of oscillation above the rated voltage, it returns to the high voltage rated voltage. The DC voltage of the low voltage side rises slightly at the low point of the first cycle, and then oscillates around the rated voltage of the low voltage. It can be seen that the oscillation amplitude remains basically unchanged, which can be understood as the reactive power of the user side does not change at this time.

more extensively globally.

C. Renewable Energy English Teaching

In English international teaching, teachers can stimulate students' interests by introducing real cases in the field of renewable energy. For instance, analyzing the development process of Tesla electric cars or exploring the successful experience of Denmark's wind industry. Through group discussions, debates, and other forms, students not only can improve their English oral and writing skills but also gain a profound understanding of renewable energy technology and its global applications.

Demand-side management strategies, such as interruptible loads, allow utility operators to temporarily reduce non-critical demand during peak times or emergencies to alleviate stress on the grid. In scenarios with high penetration of renewable energy, interruptible loads can help balance the intermittent supply of renewables through real-time response. For example, commercial buildings and industrial users can participate in interruptible load programs to obtain preferential electricity rates while providing the necessary flexibility for the grid. In highly renewable energy-penetrated power systems, interruptible loads, microgrids, and storage systems play crucial roles in providing flexibility and stability to adapt to the volatility of renewable energy. Through case studies and actual application analyses, we can not only verify the effectiveness of these strategies but also provide valuable experiences for the planning and operation of future grids. With technological advancements and market maturation, it is expected that these flexible resources will be applied

The text is based on the reality of the wind power industry and is professional. Compared with public English, wind power English has both the professional characteristics of wind power and the linguistic characteristics of English, so it is more difficult to learn, more professional, and more targeted. It is very targeted in the selection of texts. The content is not limited to the cultivation of students' English ability. It also takes into account the teaching of wind power expertise. It highlights the subject characteristics of professional English. In general, you only need to select exercises that involve transforming parts of speech. If we choose the text according to this idea, we will ignore the basic feature that "wind power professional English is built on the subject of wind power", so we can not only select the text related to parts-of-speech transformation, but also take into account the professionalism of wind science and English subject language, and select parts-of-speech transformation related to wind power technology. Each selected article follows this idea, each selected article is related to wind power in content, and the main grammar is closely integrated with the focus of unit teaching.

Therefore, foreign literature reports are rarely included directly, and most of the texts are adapted from relevant reports or translated from basic textbooks for wind power majors. Therefore, the texts are not only in line with the language of English subjects, but also in line with the actual and professional knowledge of wind power industry.

Combination of classroom teaching and online courses: Renewable energy utilization courses due to the teaching content is too much, so the use of online courses to supplement the classroom teaching is necessary. Online courses can focus on three aspects of content, the first is for boring theoretical knowledge, such as the derivation of the ideal energy output formula of wind turbines, the theoretical amount of air required for biomass combustion and the derivation of the actual smoke volume produced. These formulas are very important, but due to the class time limit can not give a detailed derivation process in class, or even if the class derivation, it is difficult for students to grasp on the spot. In this case, students watch online courses after class to supplement classroom instruction. This part of the content is only for students who have the ability to learn, and is a supplement to the classroom knowledge, such as wind turbine control and location, biomass molding compression technology, thin film solar cells and other content. Finally, for the key concepts of the course, this part of the content can be made into a micro lesson, which can be widely shared on the Internet platform, so as to facilitate students to consolidate after class.

5. Conclusion

Under the background of large-scale grid-connection of renewable energy, especially wind power, the research of traditional transmission system planning faces new challenges and opportunities. In this paper, a process optimization power flow algorithm is proposed to optimize the power system with a high proportion of renewable wind and light energy. Aiming at the low utilization rate of renewable energy optimal scheduling model, this paper puts forward the English teaching plan combined with sustainable development, and puts forward the improvement from the two aspects of textbook selection and classroom teaching. Specific conclusions are as follows:

The probability density function of fan output and photovoltaic output is obtained by wind speed and light intensity model, and the probability density function of load is also proposed. Then, interruptible load, microgrid and energy storage are used as flexible resources to improve the system's flexibility to meet the random fluctuations caused by a high proportion of wind and light, so as to maintain the stable operation of the power grid.

Process optimization trend includes time period optimization and time period succession. As the core of the process optimization power flow, the time-optimized power flow is optimized in the median cross-section, and the power balance is carried out in the two boundary value cross-sections according to the frequency modulation characteristics of the power grid and the inequality

constraints are checked. In each linear period, the optimization of the median cross-section and the cross-section check of the boundary value are organically combined to ensure the objective optimization of the process optimization flow under the process constraint.

Due to the lack of start-stop peak balancing, wind and light optimization electricity can only rely on the output of the opening unit for climbing and descending peak balancing. As a result, the peak load capacity of the wind and light-optimized power units decreases, and the units are in a state of deep peak load for a long time. The total number of deep peak loads is 390 times, which is greater than model 1, and the power abandonment cost increases. Therefore, the peak load cost, power abandonment cost and total cost of scenario 2 are all greater than model 1. It shows that reasonable arrangement of wind and light-optimized generator units to start and stop peaking is also beneficial to reduce the power abandonment cost and the total cost of the system. In this paper, the optimal scheduling of renewable energy power plants based on process optimization power flow algorithm can greatly reduce the cost.

The issue of absorbing and buffering short-term fluctuations needs further study, which could be combined with large-capacity storage technology to enhance research depth. Uncertainty power has a significant impact on the safe and stable operation of the grid; this article does not include content related to safety analysis and evaluation, which will be continued in future research work.

References

- [1] O. Ogunmodede, K. Anderson, D. Cutler, and A. Newman, "Optimizing design and dispatch of a renewable energy system," *Applied Energy*, vol. 287, p. 116527, 2021.
- [2] M. F. Ishraque, S. A. Shezan, M. M. Ali, and M. M. Rashid, "Optimization of load dispatch strategies for an islanded microgrid connected with renewable energy sources," *Applied Energy*, vol. 292, p. 116879, 2021.
- [3] Z. Z. Guo, R. L. Ye, R. Y. Liu, and J. N. Liu, "Renewable energy grid optimal scheduling strategy including pumped storage power station," (in Chinese), *Electric Power Automation Equipment*, vol. 38, no. 3, pp. 7-15, 2018.
- [4] R. F. Colmenares-Quintero *et al.*, "Learning and teaching styles in a public school with a focus on renewable energies," *Sustainability*, vol. 14, no. 23, p. 15545, 2022.
- [5] C. S. Wang, C. X. Lv, P. Li, S. Q. Li, and K. P. Zhao, "Multi-time scale model prediction and optimal scheduling for integrated energy system in a park," (in Chinese), *Proceedings of the CSEE*, vol. 39, no. 23, pp. 6791-6803, 2019.
- [6] H. Xiao, W. Pei, and L. Kong, "Multi-time scale coordinated optimal dispatch of microgrid based on model predictive control," *Automation of Electric Power Systems*, vol. 40, no. 18, pp. 7-14, 2016.
- [7] Z. F. Liu, L. L. Li, Y. W. Liu, J. Q. Liu, H. Y. Li, and Q. Shen, "Dynamic economic emission dispatch considering renewable energy generation: A novel multi-objective optimization approach," *Energy*, vol. 235, p. 121407, 2021.
- [8] W. Wei, F. Liu, and S. Mei, "Distributionally robust co-optimization of energy and reserve dispatch," *IEEE Transactions on Sustainable Energy*, vol. 7, no. 1, pp. 289-300, 2015.

- [9] Z. Li, F. Qiu, and J. Wang, "Data-driven real-time power dispatch for maximizing variable renewable generation," *Applied Energy*, vol. 170, pp. 304-313, 2016.
- [10] M. R. Chen, G. Q. Zeng, and K. D. Lu, "Constrained multi-objective population extremal optimization based economic-emission dispatch incorporating renewable energy resources," *Renewable Energy*, vol. 143, pp. 277-294, 2019.
- [11] J. Hirwa, O. Ogunmodede, A. Zolan, and A. M. Newman, "Optimizing design and dispatch of a renewable energy system with combined heat and power," *Optimization and Engineering*, pp. 1-31, 2022.
- [12] Q. Niu, M. You, Z. Yang, and Y. Zhang, "Economic emission dispatch considering renewable energy resources—A multi-objective cross entropy optimization approach," *Sustainability*, vol. 13, no. 10, p. 5386, 2021.
- [13] W. Wei, F. Liu, S. Mei, and Y. Hou, "Robust energy and reserve dispatch under variable renewable generation," *IEEE Transactions on Smart Grid*, vol. 6, no. 1, pp. 369-380, 2014.
- [14] J. Hirwa, A. Zolan, W. Becker, T. Flamand, and A. Newman, "Optimizing design and dispatch of a resilient renewable energy microgrid for a South African hospital," *Applied Energy*, vol. 348, p. 121438, 2023.
- [15] S. S. Reddy and P. R. Bijwe, "Real time economic dispatch considering renewable energy resources," *Renewable Energy*, vol. 83, pp. 1215-1226, 2015.
- [16] C. X. Guo, Y. H. Bai, X. Zheng, J. P. Zhan, and Q. H. Wu, "Optimal generation dispatch with renewable energy embedded using multiple objectives," *International Journal of Electrical Power & Energy Systems*, vol. 42, no. 1, pp. 440-447, 2012.
- [17] P. P. Biswas, P. N. Suganthan, R. Mallipeddi, and G. A. Amaratunga, "Optimal reactive power dispatch with uncertainties in load demand and renewable energy sources adopting scenario-based approach," *Applied Soft Computing*, vol. 75, pp. 616-632, 2019.
- [18] M. Zugno and A. J. Conejo, "A robust optimization approach to energy and reserve dispatch in electricity markets," *European Journal of Operational Research*, vol. 247, no. 2, pp. 659-671, 2015.
- [19] G. Wang, Y. Zha, T. Wu, J. Qiu, J. C. Peng, and G. Xu, "Cross entropy optimization based on decomposition for multi-objective economic emission dispatch considering renewable energy generation uncertainties," *Energy*, vol. 193, p. 116790, 2020.
- [20] A. Abaza, A. Fawzy, R. A. El-Schiemy, A. S. Alghamdi, and S. Kamel, "Sensitive reactive power dispatch solution accomplished with renewable energy allocation using an enhanced coyote optimization algorithm," *Ain Shams Engineering Journal*, vol. 12, no. 2, pp. 1723-1739, 2021.
- [21] E. E. Elattar, "Environmental economic dispatch with heat optimization in the presence of renewable energy based on modified shuffle frog leaping algorithm," *Energy*, vol. 171, pp. 256-269, 2019.